environmental microbiology

Environmental Microbiology (2021) **00**(00), 00–00 doi:10.1111/1462-2920.15811

# A role for PchHI as the ABC transporter in iron acquisition by the siderophore pyochelin in *Pseudomonas aeruginosa*

**Béatrice Roche**[1,2*†] **Mariel A. Garcia-Rivera**[3] **Vincent Normant**[1,2] **Lauriane Kuhn**[4] **Philippe Hammann**[4] **Mark Brönstrup**[3] **Gaëtan L. A. Mislin**[1,2] **and Isabelle J. Schalk**[1,2*]

[1]*CNRS, UMR7242, ESBS, Bld Sébastien Brant, Illkirch, F-67412, France.*

[2]*Université de Strasbourg, UMR7242, ESBS, Bld Sébastien Brant, Illkirch, F-67412, France.*

[3]*Department of Chemical Biology, Helmholtz Centre for Infection Research, Inhoffenstrasse 7, Braunschweig, 38124, Germany.*

[4]*Plateforme Protéomique Strasbourg – Esplanade, Institut de Biologie Moléculaire et Cellulaire, CNRS, FR1589, 2 allée Konrad Roentgen, Strasbourg Cedex, F-67084, France.*

## Summary

**Iron is an essential nutrient for bacterial growth but poorly bioavailable. Bacteria scavenge ferric iron by synthesizing and secreting siderophores, small compounds with a high affinity for iron. Pyochelin (PCH) is one of the two siderophores produced by the opportunistic pathogen *Pseudomonas aeruginosa*. After capturing a ferric iron molecule, PCH-Fe is imported back into bacteria first by the outer membrane transporter FptA and then by the inner membrane permease FptX. Here, using molecular biology, $^{55}$Fe uptake assays, and LC–MS/MS quantification, we first find a role for PchHI as the heterodimeric ABC transporter involved in the siderophore-free iron uptake into the bacterial cytoplasm. We also provide the first evidence that PCH is able to reach the bacterial periplasm and cytoplasm when both FptA and FptX are expressed. Finally, we detected an interaction between PchH and FptX, linking the ABC transporter PchHI with the inner permease FptX in the PCH-Fe uptake pathway. These results pave the way for a better understanding of the PCH siderophore pathway, giving future directions to tackle *P. aeruginosa* infections.**

Received 26 July, 2021; revised 10 September, 2021; accepted 5 October, 2021. *For correspondence. E-mail beatrice.roche@unibas.ch; Tel. (+41) 61 207 21 32. E-mail schalk@unistra.fr; Tel. 33 (0)3 68 85 47 19; Fax 33 (0)3 68 85 46 83. †Present address: Biozentrum, University of Basel, Basel CH-4056, Switzerland.

## Introduction

Iron is an essential nutrient for nearly all living organisms, especially bacterial pathogens facing iron-scarce environments of the host during infection (Skaar, 2010). To acquire the necessary iron, bacteria have evolved a number of strategies including the secretion of siderophores. Siderophores are small compounds produced by bacteria under iron limitation conditions. The role of siderophores is to scavenge ferric iron in the bacterial environment, and shuttle it back into the bacteria (Schalk and Guillon, 2013; Schalk and Cunrath, 2016).

In Gram-negative bacteria, outer membrane transporters (OMTs) act as the first gates for ferri-siderophore recognition and uptake. After its translocation into the periplasm, it has been reported that the ferri-siderophore complex in *Escherichia coli* is bound by a periplasmic binding protein (PBP) that is associated with an ATP-Binding Cassette (ABC) transporter (Schalk and Guillon, 2013). For the enterobactin and ferrichrome pathways in *E. coli*, two archetype siderophore-dependent iron uptake systems, the ferri-siderophores are then transported into the cytoplasm by the permease domain of the ABC transporter, coupled to ATP hydrolysis, delivering iron directly into the bacterial cytoplasm (Shea and McIntosh, 1991; Rohrbach *et al*., 1995; Zhu *et al*., 2005; Miethke *et al*., 2011). These ABC transporters are generally assembled from two separate polypeptides, each with a domain forming an inner membrane permease and a cytoplasmic nucleotide binding subunit with ATPase activity (Schalk and Guillon, 2013; Ford and Beis, 2019).

Pyoverdine (PVD), one of the two siderophores produced by the opportunistic pathogen *Pseudomonas aeruginosa*, follows a different transport mechanism. After uptake of PVD-Fe across the outer membrane by FpvA or FpvB, iron dissociates from PVD in the bacterial

periplasm, followed by the translocation of siderophore-free iron into the cytoplasm by the ABC transporter FpvDE (Schalk *et al*., 2002; Greenwald *et al*., 2009; Brillet *et al*., 2012; Ganne *et al*., 2017). Apo-PVD is recycled from the periplasm into the extracellular medium by the efflux system PvdRT-OpmQ (Imperi *et al*., 2009; Yeterian *et al*., 2010).

In addition to PVD, *P. aeruginosa* produces a second siderophore called pyochelin (PCH) (Fig. 1A) to fulfil its need for iron (Cox *et al*., 1981; Thomas, 2007). PCH chelates iron with a 2:1 (PCH:Fe) stoichiometry (Tseng *et al*., 2006), and an affinity of $10^{28}$ $M^{-2}$ (Brandel *et al*., 2012). Although PCH has a lower affinity for iron compared with the PVD, its importance should not be neglected, especially in cystic fibrosis patients where PCH plays a role in the inflammatory response (Lyczak *et al*., 2002; Hare *et al*., 2007; Cornelis and Dingemans, 2013).

The genes involved in iron acquisition by PCH are organized in three operons: *pchDCBA* (Serino *et al*., 1997), *pchEFGHI* (Reimmann *et al*., 1998, 2001) and *fptABCX* (Michel *et al*., 2007) (Fig. 1B). The *pchDCBAEFG* genes are involved in PCH biosynthesis (Serino *et al*., 1997; Reimmann *et al*., 2001), whereas *fptA* and *fptX* participate in ferri-PCH uptake with FptA as the OMT and FptX as the inner membrane transporter (Cuív *et al*., 2004; Michel *et al*., 2007; Cunrath *et al*., 2015). *fptB* and *fptC* encode proteins of unknown function, and *pchH* and *pchI* are annotated to encode a putative ABC transporter (Reimmann *et al*., 2001).

Based on previous *in vitro* experiments with the purified transcriptional regulator PchR, it was proposed that ferri-PCH acts as the intracellular effector required by PchR to activate the transcription of the genes of the PCH locus (Michel *et al*., 2005; Lin *et al*., 2013). Such a mechanism suggests that PCH enters the cytoplasm as a ferric complex, although no cellular experiments have been performed to test this hypothesis. In addition, a recent study provided evidence of more complex regulation of PCH production, with an additional level of regulation that allows PCH synthesis even in the absence of ferri-PCH in highly iron-restricted conditions (Cunrath *et al*., 2020). However, despite intensive efforts to dissect the PCH pathway, our understanding of ferri-PCH uptake is still far from complete.

Here, we investigated the role of PchH and PchI in the *P. aeruginosa* PCH pathway. A bacterial two-hybrid assay showed that (i) PchH and PchI interact with each other, and (ii) PchH interacts with FptX, linking both the heterodimeric ABC transporter PchHI with the inner membrane permease. Using $^{55}Fe$ uptake assays and LC–MS/MS-based quantification of PCH uptake, we provide (i) the first evidence that PCH (complexed with iron) enters the bacterial periplasm and cytoplasm, (ii) that FptX is involved in PCH-Fe uptake across the inner membrane and (iii) that PchHI acts as the ABC transporter to translocate siderophore-free iron into the cytoplasm.

## Results

### *PchH and PchI share classical features of ABC transporters and interact with each other*

The *PA4222* (*pchH*) and *PA4223* (*pchI*) genes are located in the *pchEFGHI* operon. The nucleotide sequences predict 570 and 574-amino acid proteins for PchH and PchI, respectively, with 35% sequence identity and 45% similarity to each other. The topology prediction indicates that both PchH and PchI are composed of an

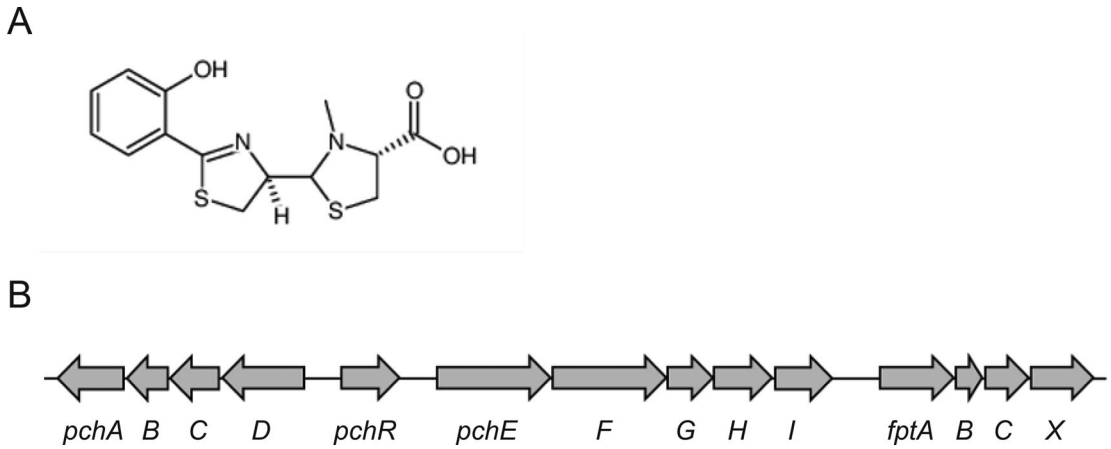


**Fig. 1.** Pyochelin structure and locus from *P. aeruginosa*. (A) Chemical structure of PCH. (B) Schematic map of the PCH locus. *pchABCDEF* are genes involved in PCH biosynthesis, *pchR* encodes a transcriptional regulator, *fptA* the PCH-Fe outer membrane transporter, *fptX* the PCH-Fe inner membrane permease and *pchH*, *pchI*, *fptB* and *fptC* proteins of unknown function.

N-terminal membrane-spanning domain and a cytoplasmic C-terminal domain (Fig. S1). It was previously reported that the PchH and PchI sequences show similarities to those of ABC transporter proteins, with the presence of the typical sequence motifs of such transporters in the C-terminal region of each of the two proteins (Kerr, 2002): the Walker A (GPSGSGKST in PchH and GPSGAGKSS in PchI) and Walker B (LLLLDEPT in PchH and PchI) motifs, both necessary for ATP binding and hydrolysis, and the ABC signature sequence LSGG involved in energy transduction (Fig. S2) (Reimmann *et al*., 2001). These features are shared with the YbtPQ ABC transporter involved in iron acquisition by the siderophore yersiniabactin in *Yersinia pestis* (Perry and Fetherston, 2011). Moreover, several bacterial ABC transporters have been reported to function as heterodimers (Fetherston *et al*., 1999; Lubelski *et al*., 2007; Torres *et al*., 2009; Yamashita *et al*., 2014; Hürlimann *et al*., 2016). We tested the ability of PchH and PchI to interact with each other, by performing a bacterial two-hybrid (BACTH) assay in *E. coli*, based on the reconstitution of adenylate-cyclase activity. The full-length *pchH* and *pchI* genes were fused to the T25/T18 domains of adenylate cyclase in the two-hybrid vectors pKT25 and pUT18C. We found that PchH interacts with PchI (Fig. 2A). Moreover, BACTH results indicate that PchH also interacts with FptX (Fig. 2B), linking both the ABC transporter and the inner membrane transporter FptX. Overall, these observations lead us to propose that PchH and PchI contain the classical features required for a heterodimeric ABC transporter in the PCH pathway, with PchH interacting somehow with the inner membrane permease FptX.

### *PchH and PchI are not involved in the regulation of the transcription or expression of the genes of the PCH pathway*

We first investigated the impact of deletion of the two genes *pchH* and *pchI*, on the transcription and expression of the various genes of the PCH pathway, using qRT-PCR and proteomic approaches. This investigation was carried on the *P. aeruginosa* wild type strain PAO1 and the corresponding Δ*pchR*, Δ*pchHI*, Δ*fptX*, Δ*fptX*Δ*pchHI* and Δ*fptA* mutants, all grown under iron-starvation conditions, for 8 h (Fig. 3). For qRT-PCR experiments, we followed the transcription of *pchR* (transcriptional regulator) and genes representative for each of the three operons *fptABCX*, *pchEFGHI* and *pchDCBA* of the PCH locus: *fptA* and *fptX*, the outer and inner membrane transporters of PCH-Fe, and *pchE* and *pchA* two enzymes involved in PCH biosynthesis.

The deletion of *pchR* had a strong inhibitory effect on the transcription of the genes of the PCH locus. As expected, the positive autoregulatory loop involving PchR was no longer active (Fig. 3A). Deletion of *fptA* and *fptX* also strongly repressed the transcription and expression of the various genes of the PCH pathway, indicating that PchR is no longer able to bind to its promoter regions (Fig. 3A and B). These data again confirm that both FptA and FptX are involved in the positive autoregulatory loop, as previously reported (Michel *et al*., 2005; Lin *et al*., 2013; Carballido Lopez *et al*., 2019) by importing into the bacteria the PCH-Fe complex interacting with PchR. Deletion of *pchH* and *pchI* had no effect on the transcription or expression of the genes of the PCH pathway, indicating that the ABC transporter PchHI plays no role in the autoregulatory loop involving PchR (Fig. 3A

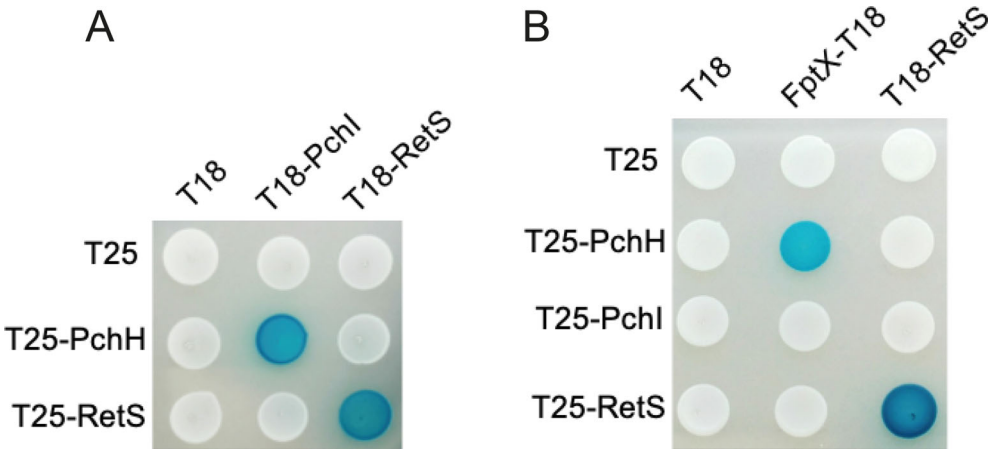


**Fig. 2.** Interactions between PchH, PchI and FptX identified by bacterial two-hybrid experiments. The *pchH*, *pchI* and *fptX* genes were cloned into the two-hybrid pKT25, pUT18C, or pUT18 vectors and the corresponding vectors used to co-transform *E. coli* DHM1 cells that were then spotted on X-gal-IPTG LB agar plates. Panel A shows the interaction between PchH and PchI and panel B that between PchH, PchI and FptX. A blue colour reflects an interaction between chimeric proteins, whereas a white colour indicates the absence of an interaction. RetS, a sensor of two-component systems, serves as the positive control (Chambonnier *et al*., 2016).

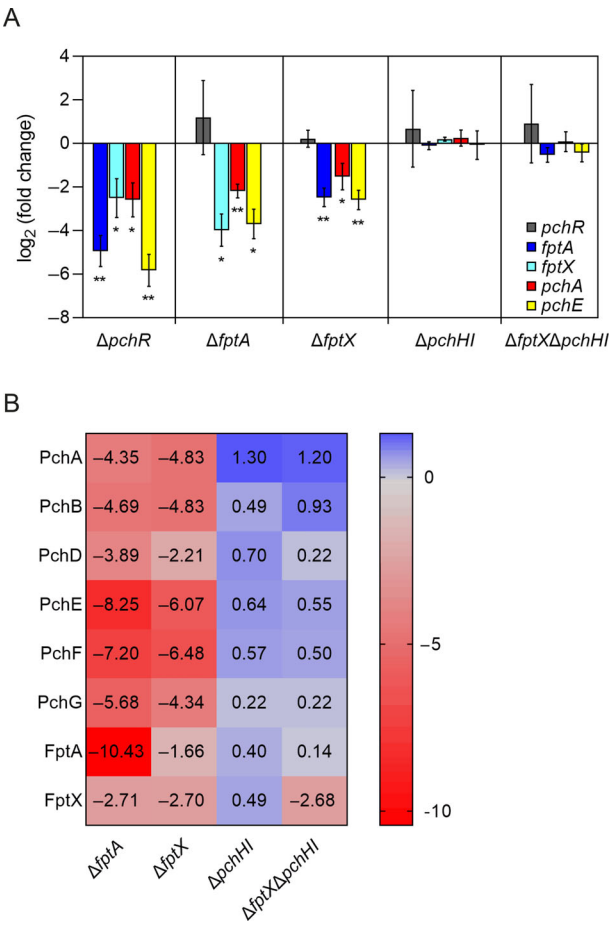


**Fig. 3.** Changes in gene transcription (panel A) and protein expression (panel B) of members of the PCH locus in *P. aeruginosa* PAO1 and mutants grown under iron-limited conditions. (A) RT-qPCR was performed on *P. aeruginosa* PAO1 and its corresponding mutants grown in CAA medium as described in section 'Experimental Procedures'. The data were normalized relative to the reference gene *uvrD* and are representative of three independent experiments performed in triplicate. Results are presented as the ratio between the values obtained for the various mutants over those obtained with PAO1 (*$P < 0.05$; **$P < 0.01$). (B) Heat map of proteins involved in the PCH pathway after proteomic analyses performed on *P. aeruginosa* PAO1 and its corresponding mutants grown in CAA medium as described in Experimental Procedures. The data are presented as the $\log_2$ fold change: the darker the shade of blue, the higher the induced expression of the protein; the darker the shade of red, the stronger the repressed expression of the protein (adjpvalue <0.05).

and B). Interestingly, the Δ*fptX*Δ*pchHI* mutant had the same phenotype as the single Δ*pchHI* mutant with PchR able to activate transcription of the PCH genes, indicating that PchR is active by an unknown mechanism even if FptX is not expressed.

In conclusion, the ABC transporter PchHI plays no role in the autoregulatory loop involving PchR: in a Δ*pchHI* mutant, all proteins of the PCH pathway (enzymes involved in PCH biosynthesis, FptA and FptX, except PchHI) are transcribed and expressed.

### *PchH and PchI do not affect the amount of PCH produced and secreted by bacteria*

As bacterial ABC transporters can export a wide variety of substrates (Davidson *et al*., 2008), we tested whether PchH and PchI participate in the production and secretion of PCH. Bacteria were grown under iron restricted conditions, pelleted, and PCH extracted from the supernatant, as described in section 'Experimental Procedures'. Consistent with previous reports (Michel *et al*., 2007), the Δ*fptA* and to a lesser extent Δ*fptX* mutants showed a strong decrease in the amount of PCH present in the growth medium (Fig. 4), consistent with low gene transcription and protein expression of enzymes involved in PCH biosynthesis in these strains (Fig. 3). The phenotype of the Δ*fptA* and Δ*fptX* mutants is consistent with the model that PCH-Fe complexes cannot enter the bacteria to activate PchR in the absence of FptA and FptX. This results in less expression of the enzymes involved in PCH biosynthesis than in the PAO1 strain, and lower amounts of produced and secreted PCH (Michel *et al*., 2007). Deletion of *pchH* and *pchI* had no detrimental effect on the amount of PCH secreted by bacteria in the growth medium, indicating that PchH and PchI are not required for PCH secretion after its synthesis in the bacterial cytoplasm. Interestingly, the triple Δ*fptX*Δ*pchHI* mutant showed a similar phenotype as the Δ*pchHI* mutant (Fig. 4). In conclusion, the ABC transporter PchHI is not involved in the secretion of newly synthesized PCH.

### *PchH and PchI are involved in iron uptake via PCH*

The ability of PchH to interact with FptX prompted us to analyse the role of PchH and PchI in iron uptake by PCH. We deleted both the *pchH* and *pchI* genes in the Δ*pvdF*Δ*pchA P. aeruginosa* strain, which is unable to synthesize the endogenous siderophores PVD and PCH. However, in this mutant the proteins of the PCH pathway are expressed (Cunrath *et al*., 2020). $^{55}$Fe uptake assays were carried out by growing the corresponding strains in iron-restricted medium followed by incubation of the bacteria in the presence of 200 nM PCH-$^{55}$Fe. After 30 min of incubation, cells were fractionated, and the radioactivity monitored in each cell compartment (Fig. 5A). The Δ*pvdF*Δ*pchA* reference strain showed a 1.8-fold higher concentration of $^{55}$Fe in the cytoplasm than the periplasm. Interestingly, the ratio of $^{55}$Fe incorporated in the periplasm and cytoplasm in the Δ*pvdF*Δ*pchA*Δ*pchHI* mutant was reversed, with a 2.5-fold higher concentration of $^{55}$Fe in the periplasm than cytoplasm (Fig. 5A). The Δ*pvdF*Δ*pchA*Δ*fptX* mutant showed a stronger ratio, with a fourfold higher concentration of $^{55}$Fe in the periplasm than in the cytoplasm, consistent with the model that

 

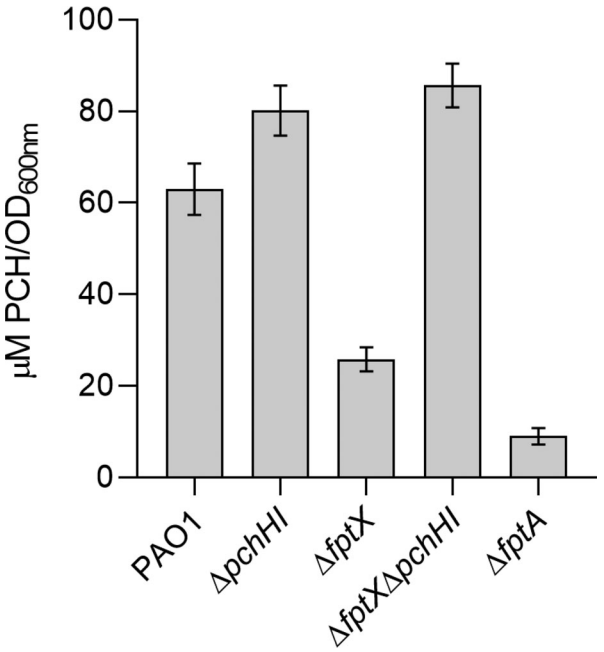


**Fig. 4.** PCH produced by PAO1 and its corresponding mutants. Cells were grown in CAA medium for 16 h at 30°C. PCH was extracted from the growth medium as described in section 'Experimental Procedures' and its concentration determined by measuring the absorbance at 320 nm. The graph shows the concentration of PCH produced for a bacterial concentration of $OD_{600\ nm}$ of 1. The error bars represent the standard deviation of six independent experiments.

FptX transports the ferri-PCH complex across the inner membrane (Cunrath *et al*., 2015). Deletion of both transporters PchHI and FptX resulted in exactly the same phenotype as that of the single *fptX* mutation (Fig. 5A).

Importantly, the highest absolute amounts of $^{55}$Fe were recovered in the extracellular medium for both the Δ*pvdF*Δ*pchA*Δ*fptA* and Δ*pvdF*Δ*pchA*Δ*fptX* mutants (Fig. S3), as no more PCH-$^{55}$Fe was imported into the bacteria in the absence of the outer and inner membrane transporters. In addition, the residual radioactivity detected in the Δ*pvdF*Δ*pchA*Δ*fptA* mutant was probably due to $^{55}$Fe contamination during cell fractionation.

In conclusion, these data highlight that the ABC transporter PchHI plays a role in iron uptake from the periplasm into the cytoplasm. Iron ions transported by PchHI can be in a complex with PCH or not.

### *Cytoplasmic localization of PCH after its uptake*

Previous studies have suggested that PCH enters the bacterial cytoplasm with iron, and that the PCH-Fe complex interacts with PchR in the auto-activation loop (Michel *et al*., 2005; Lin *et al*., 2013). Nothing is currently known about the mechanism of iron release from PCH; it may occur in the bacterial cytoplasm, at the inner membrane, or even in the periplasm. In the case of iron release in the periplasm, a fraction of PCH-Fe would enter the bacterial cytoplasm to interact with PchR and

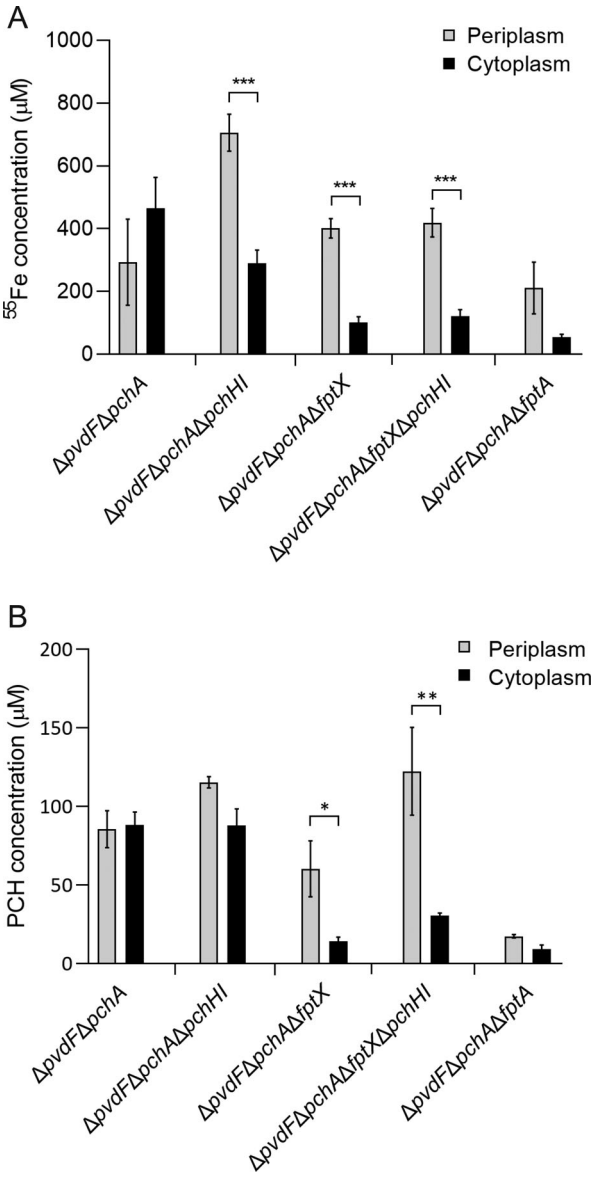


**Fig. 5.** Distribution of $^{55}$Fe (panel A) and PCH (panel B) in the *P. aeruginosa* Δ*pvdF*Δ*pchA* strain and its corresponding mutants grown under iron-restricted conditions. (A) Strains were grown in CAA medium and then incubated with PCH-$^{55}$Fe for 30 min. After incubation, the cells were pelleted, the periplasm and cytoplasm fractions isolated as described in the section 'Experimental Procedures', and the amount of $^{55}$Fe present monitored. (B) Strains were grown in CAA medium and incubated with PCH for 30 min. After incubation, the cells were pelleted, the periplasm and cytoplasm fractions isolated, and the amount of PCH was analysed by LC–MS/MS as described in Experimental Procedures.
The results are expressed in µM in the corresponding compartment. Molar concentrations in each compartment were calculated from the cellular dimensions in Table S3. The error bars represent the standard deviation of three independent experiments. Student's *t*-tests were performed (*$P < 0.05$; **$P < 0.01$; ***$P < 0.001$).

another would undergo dissociation in the periplasm. We investigated the subcellular localization of PCH by growing the Δ*pvdF*Δ*pchA* strain and the corresponding mutants under iron-starvation conditions, harvesting the cells, and incubated them in the presence of 5 μM PCH. In this assay we added only PCH and not its iron-loaded form to be as close as possible to natural conditions, in which large amounts of siderophores are produced to scavenge the environmental iron present in very low amounts. Under such conditions, PCH chelates the iron ions present in the growth medium and transports them into bacteria. Previous studies have shown that CAA medium contains approximately 20 nM iron (Schalk and Cunrath, 2016). After 30 min of incubation of the bacteria with PCH, cells were pelleted, the cell compartments isolated by cell fractionation, and the concentration of PCH in each fraction quantified by LC–MS/MS (Fig. 5B). The PCH-Fe complex appeared to be unstable in our fractionation workflow, because only PCH was detected in the biological samples, even though PCH-Fe was detectable by LC–MS in solution (Fig. S5).

In the Δ*pvdF*Δ*pchA* reference strain, PCH accumulated equally between the periplasm and cytoplasm (Fig. 5B). This observation shows for the first time that PCH can enter the bacterial cytoplasm, although it is not possible to know whether it was as the iron-free or iron-loaded form. The accumulation of periplasmic/cytoplasmic PCH was almost abolished in the Δ*fptA* mutant, showing that PCH-Fe cannot enter the cells in the absence of the outer membrane transporter FptA. The *fptX* mutation had exactly the same effect on the repartition of PCH and $^{55}$Fe between the periplasm and cytoplasm: four times more of both PCH and $^{55}$Fe accumulated in the periplasm than in the cytoplasm. This observation validates the role of FptX as the PCH-Fe inner membrane permease. Concerning the Δ*pvdF*Δ*pchA*Δ*pchHI* mutant, similar distribution of PCH was observed as for the reference strain Δ*pvdF*Δ*pchA*, with only 1.3-fold more PCH in the periplasm than cytoplasm. Deletion of both transporters, PchHI and FptX, resulted in the same phenotype as that of the single *fptX* mutation (Fig. 5B). Overall, these data suggest that the ABC transporter PchHI does not have a major role in the import into bacteria of PCH or PCH-Fe.

## Discussion

The results presented here provide new insights into the role of PchH and PchI in the *P. aeruginosa* PCH pathway. Sequence alignments clearly show that both proteins PchH and PchI contain the signature domains of ABC transporters, having both fused membrane spanning and ATPase domains, a feature shared with the YbtPQ and IrtAB ABC transporters of *Y. pestis* and *M. tuberculosis*, respectively (Rodriguez and Smith, 2006; Perry and Fetherston, 2011), both also involved in iron acquisition. In addition, PchH and PchI may function as a heterodimer transporter as suggested by their interaction revealed in our BACTH assays.

Deletion of *pchHI* had no effect on the transcription or expression of the various genes of the PCH locus: all genes of the PCH locus in a Δ*pchHI* mutant were transcribed and expressed as in PAO1 (except PchHI). Thus, PchHI plays no role in the autoregulatory loop involving PchR and activation of the transcription of the various enzymes involved in PCH synthesis. Deletion of the genes encoding the outer and inner membrane transporters FptA and FptX strongly affected transcription of the PCH locus genes, in accordance with the results of previous reports (Michel *et al*., 2007). The two proteins FptA and FptX have been proposed to import PCH-Fe complexes into the bacteria, across the outer and inner membranes, respectively. Once in the cytoplasm, the PCH-Fe complex interacts with the transcriptional regulator PchR to activate transcription of the genes of this locus (Michel *et al*., 2005; Lin *et al*., 2013; Carballido Lopez *et al*., 2019). Here, the RT-qPCR data are fully consistent with this scenario, as deletion of *fptA* or *fptX* completely abolished PchR-mediated regulation in the growth conditions used here. PchR appeared to no longer be functional in the absence of FptX. Surprisingly, in a triple Δ*fptX*Δ*pchHI* mutant, PchR appeared again to be active and able to activate transcription of the genes and expression of the proteins of the PCH pathway, as in PAO1 or in a Δ*pchHI* mutant. In a triple Δ*fptX*Δ*pchHI* mutant, no PCH-Fe was transported into the bacteria by FptX. We have shown previously that under very strong iron-restricted conditions, PchR-mediated activation of the transcription of PCH genes does not require interaction with PCH-Fe: PchR is able to interact with its promoter region in the *P. aeruginosa* genome without being in a complex with PCH-Fe (Cunrath *et al*., 2020). The situation with the Δ*fptX*Δ*pchHI* mutant appeared to be similar, with PchR becoming active even if no PCH-Fe is apparently transported into the bacteria.

After incubation of the bacteria with PCH-$^{55}$Fe, $^{55}$Fe showed more accumulation in the periplasm and less in the cytoplasm for the Δ*pvdF*Δ*pchA*Δ*pchHI* mutant than the reference strain Δ*pvdF*Δ*pchA*, highlighting a role for PchHI in iron translocation from the periplasm to the cytoplasm. However, a cytoplasmic accumulation of iron was still observed in the Δ*pchHI* mutant, suggesting that, iron must enter the cytoplasm by other means in the absence of PchH and PchI. FptX likely fulfils this function, as this transporter imports PCH-Fe able to interact with PchR, according to the work of C. Reimmann (Michel *et al*., 2005). Consistent with such a role, less $^{55}$Fe accumulated in the cytoplasm in the Δ*pvdF*Δ*pchA*Δ*fptX* mutant than the Δ*pvdF*Δ*pchA* strain. Overall, these data show that both PchHI and FptX are involved in iron transport across the inner membrane. For both the Δ*fptX* and

 

Δ*fptA* mutants, almost all $^{55}$Fe remained outside of the bacteria (Fig. S3). These data indicate that, Fe(III) cannot enter the cell via the PCH pathway in the absence of the outer or the inner membrane transporters FptA and FptX.

We also provide the first evidence of periplasmic and cytoplasmic localization of PCH using bacterial cell fractionation with LC–MS/MS-based analyses on bacteria grown under iron restricted conditions and in the presence of PCH. Such uptake certainly occurs with PCH as a PCH-Fe complex, as the bacteria have no interest in taking up the siderophore in its apo form. Almost no PCH was found inside the bacteria for the Δ*pvdF*Δ*pchA*Δ*fptA* mutant, consistent with almost no $^{55}$Fe accumulation (Fig. S3), reinforcing the fact that the PCH-Fe complex cannot enter the bacteria in the absence of FptA. As deletion of *pchH* and *pchI* did not affect PCH concentrations in the periplasm and cytoplasm relative to the reference strain Δ*pvdF*Δ*pchA*, PchHI must be dedicated to the translocation of iron that is not bound to PCH across the inner membrane. If PchHI imports siderophore-free iron across the inner membrane, dissociation of the PCH-Fe complex must occur in the bacterial periplasm. Iron release from the siderophores pyoverdine and enterobactin also occurs in the bacterial periplasm in *P. aeruginosa* cells, indicating that it is a common scenario for several iron uptake pathways of this pathogen. Moreover, if PchHI imports only PCH-free iron, we hypothesize two different fates for PCH-Fe once transported in the bacterial periplasm: a first fraction would be transported further into the cytoplasm by FptX to interact with PchR in the autoregulatory loop, and a second fraction of the PCH-Fe complexes would undergo dissociation in the bacterial periplasm by an unknown mechanism and the free iron transported further across the inner membrane into the bacterial cytoplasm by PchHI (Fig. 6).

Finally, we detected an interaction between PchH and FptX, suggesting that the ABC transporter PchHI and FptX may form a multiprotein complex. In conclusion, the combination of $^{55}$Fe with PCH uptake assays clearly demonstrate that (i) PchHI is involved in iron translocation from the periplasm to the cytoplasm, (ii) PCH is able to reach the bacterial periplasm and cytoplasm, and (iii) confirm that FptX transports PCH-Fe complexes across the inner membrane. Altogether, these data pave the way for a better understanding of the PCH siderophore pathway, giving future directions to tackle *P. aeruginosa* infections.

## Experimental procedures

### *Chemicals and growth media*

X-Gal (5-bromo-4-chloro-3-indoyl-β-D-galactopyranoside) and IPTG (Isopropyl-β-D thiogalactoside) were purchased from Euromedex (Souffelweyersheim, France). ONPG (2-Nitrophenyl-β-D galactopyranoside) was obtained from Sigma-Aldrich (Lyon, France). PCH was synthetized chemically according to previously published protocols (Youard *et al*., 2007). LB (Lennox) and LB agar medium were purchased from Difco (Franklin Lakes, New Jersey). Bacteria were grown at 30°C in LB broth or in iron-restricted medium (CAA) as previously described (Cunrath *et al*., 2015). Ampicillin (Ap; 100 μg ml$^{-1}$), kanamycin (Kan; 50 μg ml$^{-1}$), gentamicin (Gm; 30 μg ml$^{-1}$), chloramphenicol (Cm; 50 μg ml$^{-1}$) and IPTG (0.5 mM) were added when needed. The strains used in this study are listed in Table S1A.

### *Plasmid construction*

Phusion High-Fidelity DNA polymerase (ThermoFisher Scientific, Illkirch-Graffenstaden, France) was used for all PCRs using PAO1 chromosomal DNA as template. T4 DNA ligase and restriction enzymes were purchased from ThermoFisher Scientific. Oligonucleotides are listed in Table S1B. *Escherichia coli* strain Top10 was used as the host strain for all plasmids. Absence of mutations was checked by DNA sequencing. The DNA regions encoding *pchH*, *pchI* and *fptX* were amplified by PCR by using primer pairs 1235/1236, 1181/1182 and 951/952, respectively. PCR products were then digested with XbaI and KpnI enzymes and ligated into the XbaI/KpnI linearized pKT25, pKNT25, pUT18C and pUT18 vectors.

### *Deletion mutant construction*

A 500 bp DNA fragment upstream of *pchH* and a 500 bp DNA fragment downstream of *pchI* was generated using the primer pairs 1217/1219 and 1218/1220, respectively. Each PCR product was linked by overlapping PCR and products were digested with HindIII and EcoRI and cloned into the suicide vector pEXG2, yielding pEXG2Δ*pchH*Δ*pchI*. The suicide vector was transferred from *E. coli* SM10 strains into different recipient strains allowing the plasmid to integrate into the *P. aeruginosa* chromosome, with selection for gentamicin resistance. NaCl-free LB plates supplemented with 5% sucrose A were used to select the second crossing-over event. Deletions were confirmed by sequencing using external primers.

### *Bacterial two-hybrid assay*

Bacterial two-hybrid assays were performed as previously described (Battesti and Bouveret, 2012). Briefly, two compatible vectors producing proteins fused to T18 or T25 domain were co-transformed into DHM1 cells that were incubated at 30°C for 16 h. Independent colonies of each transformation were inoculated into LB medium

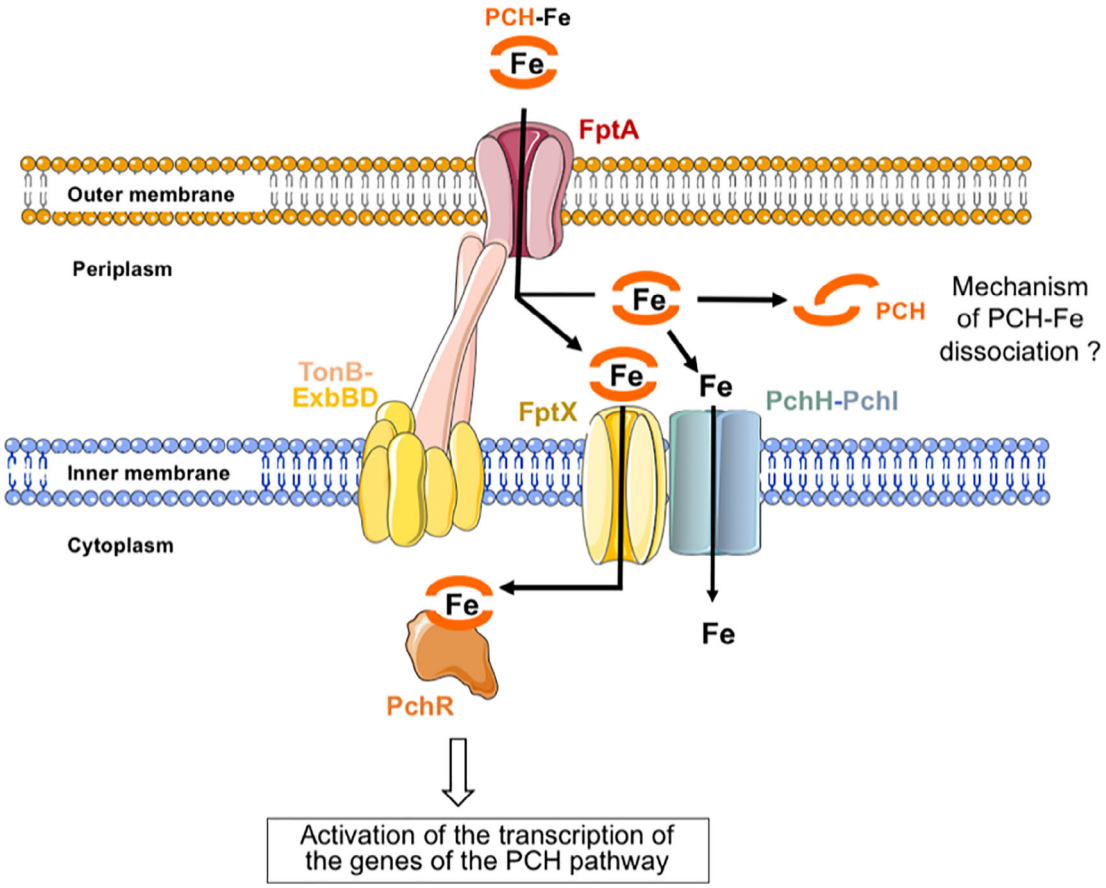


**Fig. 6.** Model of the PCH-Fe uptake pathway in *P. aeruginosa*. The PCH-Fe complexes are recognized by the outer membrane transporter FptA, allowing their translocation into the bacterial periplasm. A first fraction is transported further into the cytoplasm by FptX to interact with PchR, while a second fraction of the PCH-Fe complexes would undergo a dissociation in the bacterial periplasm by an unknown mechanism and the free iron transported further across the inner membrane into the bacterial cytoplasm by PchHI.

supplemented with ampicillin, kanamycin and 0.5 mM isopropyl β-D-1-thiogalactopyranoside (IPTG, Sigma Aldrich, Lyon, France) and incubated at 30°C for 16 h. Each culture was spotted onto LB-agar plate supplemented with appropriate antibiotics, 0.5 mM IPTG and 40 μg $ml^{-1}$ 5-bromo-4-chloro-3-indolyl-β-D-galactopyranoside (X-gal, Sigma Aldrich, Lyon, France). The plate was incubated for 16 h at 30°C.

### *Iron uptake assays and cell fractionation*

Iron uptake and cell fraction were carried out as previously described (Roche *et al*., 2021). Cells were cultured overnight in LB medium at 30°C, and afterwards at 30°C overnight in CAA medium. Then, they were diluted in fresh CAA medium and grown at 30°C overnight. Bacteria were washed with 50 mM Tris–HCl at pH 8 and diluted to an $OD_{600\ nm}$ of 1. Cells were incubated 30 min with 200 nM PCH-$^{55}$Fe at 30°C. Cells were centrifuged for 8 min at 6700*g* to obtain the supernatant (extracellular medium), and the cell pellet was resuspended in Tris-sucrose EDTA (Tris–HCl 0.2 M pH 8, EDTA 1 mM, sucrose 20%). Spheroplasts were obtained by adding 200 μg $ml^{-1}$ lysozyme (Euromedex, Souffelweryersheim, France) and incubated at 4°C for 1 h. The suspension was centrifuged for 8 min at 6700*g* at 4°C to obtain the spheroplast pellet and the periplasmic fraction (supernatant). The supernatant was ultracentrifuged (120,000*g*, 40 min, 4°C) to clarify the periplasmic fraction. Spheroplast pellet was washed with Tris–HCl 0.2 M pH 8, sucrose 20%, and resuspended in cold water by vortexing. The suspension was then incubated with benzonase for 1 h at 37°C. The cytoplasmic fraction was isolated by ultracentrifugation (120,000*g*, 40 min, 4°C). Pellet was washed twice with cold water and resuspended in Tris–HCl 0.2 M pH 8, sucrose 20% to obtain the bacterial membranes.

### *PCH production*

Determination of PCH concentration in the supernatant was performed as previously described (Roche

*et al*., 2021). Briefly, cells were cultured overnight in LB medium at 37°C, and at 30°C overnight in iron-deficient CAA medium. They were diluted to 0.1 $OD_{600nm}$ units in fresh CAA medium and incubated at 30°C for 16 h. The extracellular medium was separated from the cells by centrifugation at 7700*g* for 15 min. The supernatant was acidified by adding 1 M citric acid and PCH was extracted with dichloromethane. Pyochelin concentration was determined by measuring the absorbance at 320 nm ($\varepsilon = 4300\ l\ mol^{-1}\ cm^{-1}$). Results are expressed as a function of PCH produced (μM) to bacterial growth ($OD_{600nm}$).

### *RNA extraction and RT-qPCR analysis*

Bacteria were grown, RNA extracted, and RT-qPCR performed as previously described (Normant *et al*., 2020). Briefly, overnight cultures of *P. aeruginosa* strains grown in CAA medium were pelleted, resuspended, and diluted in fresh medium to obtain an $OD_{600nm}$ of 0.1 units. The cells were then incubated at 30°C for 8 h. An aliquot of $2.5 \times 10^8$ cells was used for RNA extraction using the RNeasy Mini kit (Qiagen). Afterwards, 1 μg of total RNA was reverse-transcribed in accordance with the manufacturer's instructions (Applied Biosystems). cDNAs were assessed in a StepOne Plus instrument (Applied Biosystems) and the appropriate primers (Table S1B) with the *uvrD* mRNA used as an internal control.

### *Proteomic analyses*

*Bacterial cultures.* PAO1 strain and its corresponding mutants were grown as described in the section 'PCH production' section. A sample of $5 \times 10^8$ cells from each culture were used for proteomic analysis. Each sample was prepared in biological triplicate.

*Mass spectrometry analysis and data post-processing.* Protein extracts were precipitated overnight with 5 volumes of cold 0.1 M ammonium acetate in 100% methanol. Proteins were then digested with sequencing-grade trypsin (Promega, Fitchburg, Massachusetts) as described previously (Normant *et al*., 2020). Each sample was further analysed by nanoLC–MS/MS on a QExactive + mass spectrometer coupled to an EASY-nanoLC-1000 (Thermo-Fisher Scientific, USA). Data were searched against the *Pseudomonas aeruginosa* UniprotKB subdatabase with a decoy strategy (UniprotKB release 2016_12, taxon 208964, *Pseudomonas aeruginosa* strain PAO1, 5564 forward protein sequences). Peptides and proteins were identified with Mascot algorithm (version 2.5.1, Matrix Science, London, UK) and data were further imported into Proline v1.4 software (http://proline.profiproteomics.fr/). Proteins were validated on Mascot pretty rank equal to 1%, and 1% FDR on both peptide spectrum matches (PSM score) and protein sets (Protein Set score). The total number of MS/MS fragmentation spectra was used to relatively quantify each protein (Spectral Count relative quantification). Proline was further used to align the Spectral Count values across all samples. The total number of MS/MS fragmentation spectra was used to quantify each protein from at least three independent biological replicates. After a column-wise normalization of the data matrix, the spectral count values were submitted to a negative-binomial test using an edgeR GLM regression through R (R v3.2.5). For each identified protein, an adjusted *P*-value (adjp) corrected by Benjamini–Hochberg was calculated, as well as a protein fold-change (FC). The mass spectrometric data were deposited to the ProteomeXchange Consortium via the PRIDE partner repository with the dataset identifier PXD026833.

### *Bacterial subcellular localization of PCH*

*Bacterial culture and fractionation.* Cells were cultured and fractionated as described in the iron uptake assays and cell fractionation section (Roche *et al*., 2021), except that cells were incubated with 5 μM PCH. Subcellular fraction each of 200 μl was precipitated by mixing with 200 μl formic acid 0.1 M and 500 μl acetonitrile/methanol (1:1). Suspension was centrifuged (10,000*g*, 1 h, 4°C) and the supernatant was kept and frozen at –80°C for LC–MS/MS analysis.

*LC–MS/MS analysis.* The analytical protocol was similar to the one reported by Prochnow *et al*. (2019). A multi-reaction monitoring method (MRM) was developed for PCH in an AB Sciex QTrap 6500 triple quadrupole mass spectrometer (AB Sciex, Darmstadt, Germany). A positively charged precursor ion was mass-selected and submitted to collision-induced fragmentation, and the resulting product ions were scanned to identify the two most abundant fragments for subsequent MRM experiments. The transition to the first fragment ion (T1) is considered as the quantifier fragment (used for calculations of peak area vs. concentration), and the transition to second fragment ion (T2) is considered as the qualifier (confirmation of the original precursor ion). Caffeine was included in the MRM as an internal standard (ISTD), so the method monitored in total four transitions: two for PCH and two for caffeine (Table S2).

The samples containing the subcellular fractions were concentrated overnight using a centrifugal vacuum concentrator at 20°C coupled to a cold trap at −50°C (both from Labconco Corporation, Kansas, Missouri). The dry remnants were reconstituted in 200 μl of ACN:$H_2O$ 1:1 + 0.1% formic acid +10 ng $ml^{-1}$ caffeine as ISTD

(LC–MS solution). The samples were analysed with a ZORBAX Eclipse Plus C18 2.1 mm × 50 mm reverse phase column with 1.8 μm pore size on an Agilent 1290 UHPLC (Agilent Technologies, Santa Clara, California), coupled to the triple quadrupole mass spectrometer. The corresponding mass transitions for PCH and ISTD were monitored simultaneously at a constant flow rate of 700 μl $min^{-1}$ with a linear gradient elution from 99% eluent A (water with 0.1% v/v formic acid) to 99% eluent B (acetonitrile with 0.1% v/v formic acid) within 6 min. The samples of periplasmic and membrane fractions contained a solid sucrose residue after drying, but not the cytoplasmic fraction, which increased the final volumes when resuspended in the LC–MS solution. To correct for this dilution difference, a normalization by the ISTD peak areas in every sample was carried out as follows: Normalized PCH peak area of the sample = PCH peak area of the sample × maximum ISTD peak area of all samples/ISTD peak area of the sample. Standard curves were obtained by measuring predefined concentrations of PCH prepared in the LC–MS solution. The integrated peak areas were then plotted over PCH concentration in micromolar, and a linear regression curve was performed by least squares. The amount of PCH in subcellular fractions was determined on the basis of the regression curve and the sample volume of 200 μl (Fig. S4).

### *Significance tests*

Student's *t* test was used for two-group comparisons using unpaired two-tailed *t* test. Analyses were performed using GraphPad Prism 8.

## ACKNOWLEDGEMENTS

Authors acknowledge the Centre National de la Recherche Scientifique (CNRS) for general financial support. BR would like to thank Roche Pharmaceutical Research and Early Development Basel for their financial support via the Roche Postdoctoral Fellowship (RPF) Program. We thank Aurélia Battesti (LCB, Marseille) for kindly providing the empty two-hybrid vectors. The mass spectrometry instrumentation was funded by the University of Strasbourg, IdEx 'Equipement mi-lourd' 2015. We also received support by a grant from the Joint Programming Initiative on Antimicrobial Resistance (JPI AMR, grant number: 01K11825).

## References

Battesti, A., and Bouveret, E. (2012) The bacterial two-hybrid system based on adenylate cyclase reconstitution in *Escherichia coli*. *Methods* **58**: 325–334. https://doi.org/10.1016/j.ymeth.2012.07.018.

Brandel, J., Humbert, N., Elhabiri, M., Schalk, I.J., Mislin, G. L.A., and Albrecht-Gary, A.-M. (2012) Pyochelin, a siderophore of *Pseudomonas aeruginosa*: physicochemical characterization of the iron(III), copper(II) and zinc(II) complexes. *Dalton Trans* **41**: 2820–2834. https://doi.org/10.1039/c1dt11804h.

Brillet, K., Ruffenach, F., Adams, H., Journet, L., Gasser, V., Hoegy, F., *et al*. (2012) An ABC transporter with two periplasmic binding proteins involved in iron acquisition in *Pseudomonas aeruginosa*. *ACS Chem Biol* **7**: 2036–2045. https://doi.org/10.1021/cb300330v.

Carballido Lopez, A., Cunrath, O., Forster, A., Pérard, J., Graulier, G., Legendre, R., *et al*. (2019) Non-specific interference of cobalt with siderophore-dependent iron uptake pathways. *Metallomics* **11**: 1937–1951.

Chambonnier, G., Roux, L., Redelberger, D., Fadel, F., Filloux, A., Sivaneson, M., *et al*. (2016) The hybrid histidine kinase LadS forms a multicomponent signal transduction system with the GacS/GacA two-component system in *Pseudomonas aeruginosa*. *PLoS Genet* **12**: e1006032. https://doi.org/10.1371/journal.pgen.1006032.

Cornelis, P., and Dingemans, J. (2013) *Pseudomonas aeruginosa* adapts its iron uptake strategies in function of the type of infections. *Front Cell Infect Microbiol* **14**: 75. https://doi.org/10.3389/fcimb.2013.00075.

Cox, C.D., Rinehart, K.L., Moore, M.L., and Cook, J.C. (1981) Pyochelin: novel structure of an iron-chelating growth promoter for Pseudomonas aeruginosa. *Proc Natl Acad Sci U S A* **78**: 4256–4260. https://doi.org/10.1073/pnas.78.7.4256.

Cuív, P.O., Clarke, P., Lynch, D., and O'Connell, M. (2004) Identification of rhtX and fptX, novel genes encoding proteins that show homology and function in the utilization of the siderophores rhizobactin 1021 by Sinorhizobium meliloti and pyochelin by Pseudomonas aeruginosa, respectively. *J Bacteriol* **186**: 2996–3005. https://doi.org/10.1128/jb.186.10.2996-3005.2004.

Cunrath, O., Gasser, V., Hoegy, F., Reimmann, C., Guillon, L., and Schalk, I.J. (2015) A cell biological view of the siderophore pyochelin iron uptake pathway in Pseudomonas aeruginosa. *Environ Microbiol* **17**: 171–185. https://doi.org/10.1111/1462-2920.12544.

Cunrath, O., Graulier, G., Carballido-Lopez, A., Pérard, J., Forster, A., Geoffroy, V.A., *et al*. (2020) The pathogen *Pseudomonas aeruginosa* optimizes the production of the siderophore pyochelin upon environmental challenges. *Metallomics* **12**: 2108–2120. https://doi.org/10.1039/d0mt00029a.

Davidson, A.L., Dassa, E., Orelle, C., Chen, J. (2008) Structure, function, and evolution of bacterial ATP-binding cassette systems. *Microbiol Mol Biol Rev* **72**: 317–364, table of contents. doi: https://doi.org/10.1128/MMBR.00031-07

Fetherston, J.D., Bertolino, V.J., and Perry, R.D. (1999) YbtP and YbtQ: two ABC transporters required for iron uptake in Yersinia pestis. *Mol Microbiol* **32**: 289–299.

Ford, R.C., and Beis, K. (2019) Learning the ABCs one at a time: structure and mechanism of ABC transporters. *Biochem Soc Trans* **47**: 23–36. https://doi.org/10.1042/BST20180147.

Ganne, G., Brillet, K., Basta, B., Roche, B., Hoegy, F., Gasser, V., and Schalk, I.J. (2017) Iron release from the siderophore pyoverdine in *Pseudomonas aeruginosa* involves three new actors: FpvC, FpvG, and FpvH. *ACS Chem Biol* **12**: 1056–1065. https://doi.org/10.1021/acschembio.6b01077.

Greenwald, J., Nader, M., Celia, H., Gruffaz, C., Geoffroy, V., Meyer, J.-M., *et al*. (2009) FpvA bound to non-cognate pyoverdines: molecular basis of siderophore recognition by an iron transporter. *Mol Microbiol* **72**: 1246–1259. https://doi.org/10.1111/j.1365-2958.2009.06721.x.

Hare, N.J., Soe, C.Z., Rose, B., Harbour, C., Codd, R., Manos, J., and Cordwell, S.J. (2007) Proteomics of *Pseudomoas aeruginosa* Australian epidemic strain 1 (AES-1) cultured under conditions mimicking the cystic fibrosis lung reveals increased iron acquisition via the siderophore pyochelin. *J Proteome Res* **11**: 776–795. https://doi.org/10.1021/pr200659h.

Hürlimann, L.M., Corradi, V., Hohl, M., Bloemberg, G.V., Tieleman, D.P., and Seeger, M.A. (2016) The heterodimeric ABC transporter EfrCD mediates multidrug efflux in *Enterococcus faecalis*. *Antimicrob Agents Chemother* **60**: 5400–5411. https://doi.org/10.1128/AAC.00661-16.

Imperi, F., Tiburzi, F., and Visca, P. (2009) Molecular basis of pyoverdine siderophore recycling in *Pseudomonas aeruginosa*. *Proc Natl Acad Sci U S A* **106**: 20440–20445. https://doi.org/10.1073/pnas.0908760106.

Kerr, I.D. (2002) Structure and association of ATP-binding cassette transporter nucleotide-binding domains. *Biochim Biophys Acta* **1561**: 47–64. https://doi.org/10.1016/s0304-4157(01)00008-9.

Lin, P.-C., Youard, Z.A., and Reimmann, C. (2013) In vitro-binding of the natural siderophore enantiomers pyochelin and enantiopyochelin to their AraC-type regulators PchR in Pseudomonas. *Biometals* **26**: 1067–1073. https://doi.org/10.1007/s10534-013-9676-5.

Lubelski, J., Konings, W.N., and Driessen, A.J.M. (2007) Distribution and physiology of ABC-type transporters contributing to multidrug resistance in bacteria. *Microbiol Mol Biol Rev* **71**: 463–476. https://doi.org/10.1128/MMBR.00001-07.

Lyczak, J.B., Cannon, C.L., and Pier, G.B. (2002) Lung infections associated with cystic fibrosis. *Clin Microbiol Rev* **15**: 194–222. https://doi.org/10.1128/CMR.15.2.194-222.2002.

Michel, L., Bachelard, A., and Reimmann, C. (2007) Ferripyochelin uptake genes are involved in pyochelin-mediated signalling in *Pseudomonas aeruginosa*. *Microbiology (Reading)* **153**: 1508–1518. https://doi.org/10.1099/mic.0.2006/002915-0.

Michel, L., González, N., Jagdeep, S., Nguyen-Ngoc, T., and Reimmann, C. (2005) PchR-box recognition by the AraC-type regulator PchR of Pseudomonas aeruginosa requires the siderophore pyochelin as an effector. *Mol Microbiol* **58**: 495–509. https://doi.org/10.1111/j.1365-2958.2005.04837.x.

Miethke, M., Hou, J., and Marahiel, M.A. (2011) The siderophore-interacting protein YqjH acts as a ferric reductase in different iron assimilation pathways of Escherichia coli. *Biochemistry* **50**: 10951–10964. https://doi.org/10.1021/bi201517h.

Normant, V., Josts, I., Kuhn, L., Perraud, Q., Fritsch, S., Hammann, P., *et al*. (2020) Nocardamine-dependent iron uptake in *Pseudomonas aeruginosa*: exclusive involvement of the FoxA outer membrane transporter. *ACS Chem Biol* **15**: 2741–2751. https://doi.org/10.1021/acschembio.0c00535.

Perry, R.D., and Fetherston, J.D. (2011) Yersiniabactin iron uptake: mechanisms and role in *Yersinia pestis* pathogenesis. *Microbes Infect* **13**: 808–817. https://doi.org/10.1016/j.micinf.2011.04.008.

Prochnow, H., Fetz, V., Hotop, S.-K., García-Rivera, M.A., Heumann, A., and Brönstrup, M. (2019) Subcellular quantification of uptake in gram-negative bacteria. *Anal Chem* **91**: 1863–1872. https://doi.org/10.1021/acs.analchem.8b03586.

Reimmann, C., Patel, H.M., Serino, L., Barone, M., Walsh, C.T., and Haas, D. (2001) Essential PchG-dependent reduction in pyochelin biosynthesis of *Pseudomonas aeruginosa*. *J Bacteriol* **183**: 813–820. https://doi.org/10.1128/JB.183.3.813-820.2001.

Reimmann, C., Serino, L., Beyeler, M., and Haas, D. (1998) Dihydroaeruginoic acid synthetase and pyochelin synthetase, products of the pchEF genes, are induced by extracellular pyochelin in *Pseudomonas aeruginosa*. *Microbiology (Reading)* **144**: 3135–3148. https://doi.org/10.1099/00221287-144-11-3135.

Roche, B., Mislin, G.L.A., and Schalk, I.J. (2021) Identification of the fatty acid coenzyme-A ligase FadD1 as an interacting partner of FptX in the *Pseudomonas aeruginosa* pyochelin pathway. *FEBS Lett* **595**: 370–378. https://doi.org/10.1002/1873-3468.14012.

Rodriguez, G.M., and Smith, I. (2006) Identification of an ABC transporter required for iron acquisition and virulence in *Mycobacterium tuberculosis*. *J Bacteriol* **188**: 424–430. https://doi.org/10.1128/JB.188.2.424-430.2006.

Rohrbach, M.R., Braun, V., and Köster, W. (1995) Ferrichrome transport in Escherichia coli K-12: altered substrate specificity of mutated periplasmic FhuD and interaction of FhuD with the integral membrane protein FhuB. *J Bacteriol* **177**: 7186–7193. https://doi.org/10.1128/jb.177.24.7186-7193.1995.

Schalk, I.J., Abdallah, M.A., and Pattus, F. (2002) Recycling of pyoverdin on the FpvA receptor after ferric pyoverdin uptake and dissociation in *Pseudomonas aeruginosa*. *Biochemistry* **41**: 1663–1671. https://doi.org/10.1021/bi0157767.

Schalk, I.J., and Cunrath, O. (2016) An overview of the biological metal uptake pathways in *Pseudomonas aeruginosa*. *Environ Microbiol* **18**: 3227–3246. https://doi.org/10.1111/1462-2920.13525.

Schalk, I.J., and Guillon, L. (2013) Fate of ferrisiderophores after import across bacterial outer membranes: different iron release strategies are observed in the cytoplasm or periplasm depending on the siderophore pathways. *Amino Acids* **44**: 1267–1277. https://doi.org/10.1007/s00726-013-1468-2.

Serino, L., Reimmann, C., Visca, P., Beyeler, M., Chiesa, V.D., and Haas, D. (1997) Biosynthesis of pyochelin and dihydroaeruginoic acid requires the iron-regulated pchDCBA operon in *Pseudomonas aeruginosa*. *J Bacteriol* **179**: 248–257. https://doi.org/10.1128/jb.179.1.248-257.1997.

Shea, C.M., and McIntosh, M.A. (1991) Nucleotide sequence and genetic organization of the ferric enterobactin transport system: homology to other periplasmic binding

protein-dependent systems in *Escherichia coli*. *Mol Microbiol* **5**: 1415–1428. https://doi.org/10.1111/j.1365-2958.1991.tb00788.x.

Skaar, E.P. (2010) The battle for iron between bacterial pathogens and their vertebrate hosts. *PLoS Pathog* **6**: e1000949. https://doi.org/10.1371/journal.ppat.1000949.

Thomas, M.S. (2007) Iron acquisition mechanisms of the *Burkholderia cepacia* complex. *Biometals* **20**: 431–452. https://doi.org/10.1007/s10534-006-9065-4.

Torres, C., Galián, C., Freiberg, C., Fantino, J.-R., and Jault, J.-M. (2009) The YheI/YheH heterodimer from *Bacillus subtilis* is a multidrug ABC transporter. *Biochim Biophys Acta* **1788**: 615–622. https://doi.org/10.1016/j.bbamem.2008.12.012.

Tseng, C.-F., Burger, A., Mislin, G.L.A., Schalk, I.J., Yu, S. S.-F., Chan, S.I., and Abdallah, M.A. (2006) Bacterial siderophores: the solution stoichiometry and coordination of the Fe(III) complexes of pyochelin and related compounds. *J Biol Inorg Chem* **11**: 419–432. https://doi.org/10.1007/s00775-006-0088-7.

Yamashita, M., Sheperd, M., Booth, W.I., Xie, H., Postis, V., *et al*. (2014) Structure and function of the bacterial heterodimeric ABC transporter CydDC: stimulation of ATPase activity by thiol and heme compounds. *J Biol Chem* **289**: 23177–23188. https://doi.org/10.1074/jbc.M114.590414.

Yeterian, E., Martin, L.W., Lamont, I.L., and Schalk, I.J. (2010) An efflux pump is required for siderophore recycling by *Pseudomonas aeruginosa*. *Environ Microbiol Rep* **2**: 412–418. https://doi.org/10.1111/j.1758-2229.2009.00115.x.

Youard, Z.A., Mislin, G.L.A., Majcherczyk, P.A., Schalk, I.J., and Reimmann, C. (2007) *Pseudomonas fluorescens* CHA0 produces enantio-pyochelin, the optical antipode of the *Pseudomonas aeruginosa* siderophore pyochelin. *J Biol Chem* **282**: 35546–35553. https://doi.org/10.1074/jbc.M707039200.

Zhu, M., Valdebenito, M., Winkelmann, G., and Hantke, K. (2005) Functions of the siderophore esterases IroD and IroE in iron-salmochelin utilization. *Microbiology (Reading)* **151**: 2363–2372. https://doi.org/10.1099/mic.0.27888-0.

## Supporting Information

Additional Supporting Information may be found in the online version of this article at the publisher's web-site:

**Table S1.** Strains, plasmids and oligonucleotides used in this study.

A. Strains and plasmids used in this study.
B. Oligonucleotides used in this study.

**Table S2.** Transitions monitored in targeted methods.

**Table S3.** Measurements of dimensions and compartments of *P. aeruginosa*.

A. Cellular dimensions (from Steinberger *et al*., 2002; Matias *et al*., 2003).

**Fig. S1.** Topology model for the *P. aeruginosa* PchH (A) and PchI (B) proteins at the inner membrane (IM). The six-transmembrane segments predicted using the CCTOP algorithm are shown with their membrane boundaries (in blue).

**Fig. S2.** Comparison of the C-terminal amino acid sequences between YbtP, YbtQ, PchH and PchI. The polypeptide sequences of PchH (GI 12668020), PchI (GI 12668018), YbtP (GI 4106633) and YbtQ (GI 4106632) were used to perform local alignment with Clustal omega. Identical, highly conserved and semi-conserved amino acids are identified by '*', ':'; '.', respectively. The bracketed sequences indicate the ABC transporter domains and the numbers denote the amino-acid position in each protein. The three boxed regions indicated the conserved motifs: Walker A, ABC signature, and Walker B.

**Fig. S3.** Amount of $^{55}$Fe in the *P. aeruginosa* Δ*pvdF*Δ*pchA* strain and its corresponding mutants grown under iron-limited conditions. Strains were grown in CAA medium and then incubated with 200 nM PCH-$^{55}$Fe for 30 min. The cells were pelleted and the extracellular medium and membrane fractions isolated to monitor the amount of $^{55}$Fe in each strain as described in Experimental Procedures. The error bars represent the standard deviation of three independent experiments.

**Fig. S4.** Calibration curve for pure PCH in LC–MS solvent. Peak areas correspond to the most abundant transition T1: 325.1 → 190.2

**Fig. S5.** MS spectra of PCH:Fe complexes detected by Q-TOF. PCH (500 μM) was incubated with 250 μM Fe(III) for 15 min at room temperature and detected by LC-coupled Q-TOF mass spectrometry. The three most intense ions correspond to the monochelate PCH:Fe, and the bischelate 2PCH:Fe and its sodiated adduct, in agreement with previous characterization of ferric complexes (Brandel *et al*., 20122012).